Surface enhanced luminescence and Raman scattering from ferroelectrically defined Ag nanopatterned arrays

Signe Damm,[1] N. Craig Carville,[1] Michele Manzo,[2] Katia Gallo,[2] Sergio G. Lopez,[3] Tia E. Keyes,[3] Robert J. Forster,[3] Brian J. Rodriguez,[1] and James H. Rice[1]
[1]*School of Physics, University College Dublin, Belfield, Dublin 4, Ireland*
[2]*Department of Applied Physics, KTH – Royal Institute of Technology, 106 91 Stockholm, Sweden*
[3]*School of Chemical Science, Dublin City University, Dublin, Ireland*

(Received 20 June 2013; accepted 1 August 2013; published online 20 August 2013; corrected 21 August 2013)

Ag nanopatterned arrays prepared using periodically proton exchanged templates have been demonstrated to support surface enhanced luminescence. Fluorescence lifetime imaging reveals that luminescence intensity is greatest on Ag and that the lifetime of the molecular probe is reduced, in line with a surface enhanced luminescence mechanism. Studies establish that the substrate simultaneously supports surface enhanced luminescence and Raman scattering. Spatial dependence along the nanopatterned arrays shows <7% variation in Raman scattering signal intensity, offering high reproducibility for practical applications. Fluorophores emitting near the plasmon absorption maxima are enhanced 4-fold. © *2013 AIP Publishing LLC*. [http://dx.doi.org/10.1063/1.4818910]

Metallic nanostructures made from metals such as silver or gold yield plasmons when light creates a collective oscillation of the conduction electrons on the surface of the metal.[1–7] The characteristic properties of the plasmonic structures have been found to be greatly dependent on factors such as size, shape, and dielectric environment.[2–7] Constructing specific patterns or architectures of plamonic active materials with nanoscale control and feature size is of interest in a variety of plasmonic applications ranging from sensing to enhanced fluorescence.[1,2]

Self-assembly is the spontaneous and reversible organization of particulate units (e.g., molecules or nanoparticles) into higher ordered structures,[8,9] which has been applied to produce a wide range of materials with nanometer sized features such as one dimensional quantum wires or zero dimensional quantum dots.[10–14] One application of self-assembly is to make precisely patterned materials that possess well defined properties by organising particles with specific physical properties via external directing (e.g., electric) fields.[15] Ferroelectric lithography is an approach based on patterning the spontaneous polarization inside ferroelectric crystals so as to engineer static electric field distributions, suitable for driving bottom-up assembly and nanodeposition at the surface of ferroelectric templates.[16] Besides electric field poling,[17] the spontaneous polarization in materials such as $LiNbO_3$, can be modified through the chemical process of proton exchange.[18] This method accounts for a change in crystal lattice of the ferroelectric substrate creating a modification to the polarization and charge at the surface. This is an emerging method that enables directed self-assembly, which potentially offers a cost effective way to create arrays of metallic nanostructures.[6,19] This approach has the potential to enable control of surface self-assembly processes with nanoscale precision over mm to cm lateral sample sizes and beyond, making such an approach applicable to engineer plasmonic devices.

Proton exchange-based and more traditional ferroelectric lithography-based methods have been applied to direct self-assembly of Ag nanoparticles to form a number of different nano- and microstructured materials.[15,19–25] Studies have shown that metallic nanoparticle deposition from an aqueous solution onto +Z surfaces of $LiNbO_3$ domain patterns can be achieved.[23–25] The nanopatterned features created using Ag nanoparticles possessed a uniform distribution with a size variation between 2 and 10 nm in both diameter and height.[24] Photochemical reduction on $LiNbO_3$ has been shown under certain conditions to result in nanopatterns which form along domain walls,[17] which have further been shown to be conducting.[26] Dunn and Tiwari have demonstrated photochemical reduction on both +Z and −Z surfaces, and have demonstrated that the power of the irradiation is a critical parameter.[27] Sun *et al*. have further reported on the dependence of the wavelength of the light and of the concentration of the solution.[28]

Chemical patterning potentially offers a method to create substrates that support reproducible surface enhanced Raman scattering spectroscopy (SERS) via arrays of nanopatterns made from Ag nanoparticles.[19,22] Damm *et al*. demonstrated using a molecular probe 4-Aminothiophenol (4-ABT) absorbed onto a Ag nanopatterned array that SERS can be obtained. The authors showed that the observed SERS spectra show peaks arising from b_2 modes, which occur for plasmon enhanced Raman scattering from 4-ABT, in place of a_1 modes, which occur in normal Raman scattering.[22] We study here Ag nanopatterned arrays formed using Ferroelectric lithography based on periodically proton exchanged (PPE) template methods.[29] We demonstrate that the resulting Ag nanopatterned arrays support both SERS and surface enhancement of luminescence (SEL).

The Ag nanopatterned arrays reported here were made using PPE templates. The methodology to create the nanopatterned arrays has been outlined previously.[19,22] Briefly, the Ag is deposited by photochemical reduction in solution under UV irradiation along the boundaries between ferroelectric regions of the substrate (see Figs. 1(a-i) and 1(a-ii)) where the electric field magnitude is at maximum, creating

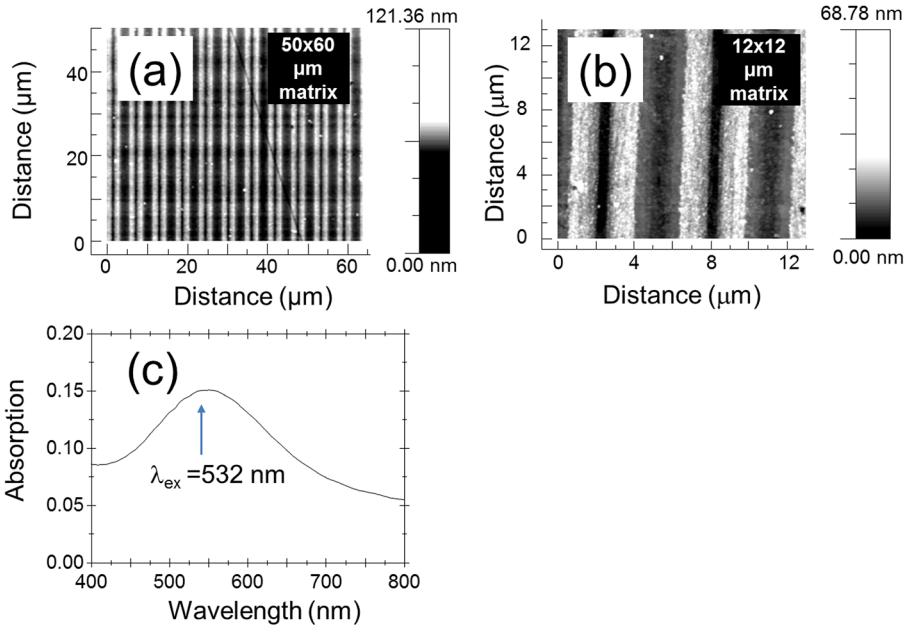

FIG. 1. (a) and (b) AFM topography image of the substrate showing the presence of well-defined stripes of Ag nanopatterned arrays. (c) Optical absorption spectrum of the Ag array-patterned substrate.

nanopatterned arrays. The samples were cleaned prior to deposition of Ag by sonication for 10 min each in isopropanol, acetone, and Milli-Q water. After 150 μl of 10^{-2} M concentration $AgNO_3$ solution was pipetted onto the substrate the samples were illuminated. The photogenerated electrons lead to selective deposition of Ag particles on the ferroelectric template through a reduction reaction.[19] The samples were subsequently rinsed in Milli-Q water for 1 min and blown dry with compressed nitrogen.

Two probe molecules were used to investigate the plasmon properties of the nanopatterned arrays. A monolayer of Rhodamine 6G (Rh6G) was prepared by dipping the sample in 0.01 mM H_2O solution of Rh6G for 24 h, following 5 min in H_2O to wash off any excess probe molecules. A monolayer of $[Ru(bpy)_2(Qbpy)]^{2+}$ (Rubpy) was prepared by dipping the samples in 6 mM MeOH solution of Rubpy for 10 min, following 1 min in MeOH to wash off any excess molecules. The samples were illuminated with visible light through a 50× objective lens, and the Raman scattering signals were collected at a backscattered angle and directed onto a charge coupled device (CCD) via a monochromator.[3–7] The setup for the Raman scattering studies on the PPE sample was with laser power = 25 mW and excitation wavelength $\lambda_{ex} = 532$ nm.

Figs. 1(a) and 1(b) show AFM images of the array-patterned substrate. The AFM topography image shows the presence of multiple arrays of Ag (a nanopatterned array). The size of the Ag linear structure is ca. 1000 nm wide and 50 nm in height. The length of the Ag linear structure is $\gg 10$ μm. The Ag linear structures possess additional nano-sized fine-structure arising from the presence of small (ca. 40 nm) sized Ag nanoparticles that are assembled to form the larger Ag linear structures.

The optical absorption spectrum of the Ag nanopatterned array is shown in Fig. 1(c). The absorption spectrum shows broad absorption with $\lambda_{\text{max absorption}}$ ca. 550 nm. Raman scattering spectroscopy of the array substrate was performed on $LiNbO_3$ + Ag nanopattern + Rh6G. The resulting Raman scattering spectrum is shown in Fig. 2(a). The Raman scattering spectrum was recorded by placing the excitation laser over the metallic pattern with the probe molecule present. The Raman scattering spectrum in Fig. 2(a-α) (displaying only the region above 1000 cm^{-1}) shows several strong Raman scattering bands between ca. 1200 and 1700 cm^{-1}. Raman scattering bands for $LiNbO_3$ occur only below 1000 cm^{-1}.[19,22] On this basis, the observed Raman scattering bands are assigned to the probe molecule. The observed Raman scattering bands match all the observed spectral features for the probe molecule.[5–7] Recording the Raman scattering off the silver by positioning the probe laser away from the Ag nanopatterned arrays, probing only the $LiNbO_3$ substrate + Rh6G was also performed. The resulting Raman scattering spectrum is shown in

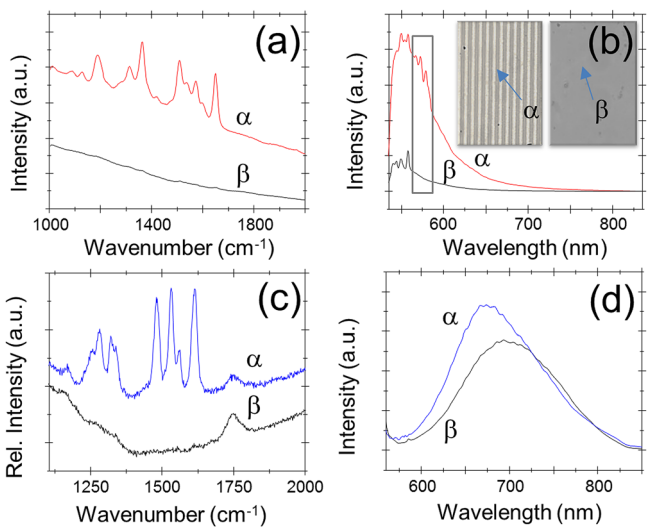

FIG. 2. (a) Raman scattering spectrum from Rh6G: α (SERS) on Ag and β off Ag on the $LiNbO_3$ substrate. (b) Luminescence (with Raman scattering spectrum superimposed) from Rh6G: α on Ag and β off Ag on the $LiNbO_3$ substrate. Insets show optical transmission microscopy images recorded the same time the spectra in (b) were taken. (c) Raman scattering from Rubpy: α (SERS) on Ag and β off Ag on the $LiNbO_3$ substrate. (d) Luminescence from Rubpy: α on Ag and β off Ag on the $LiNbO_3$ substrate.

Fig. 2(a-β) and this shows the presence of negligible peak intensity present on the background compared to when Ag is present, indicating that the Ag enhances the Raman scattering efficiently, i.e., SERS is observed for the probe molecule on the Ag.

The luminescence property of the array substrate was subsequently probed. Luminescence spectroscopy studies of $LiNbO_3$ + Ag nanopattern + Rh6G sample were undertaken. The resulting luminescence spectrum is shown in Fig. 2(b). The luminescence spectrum was recorded by placing the excitation laser over a metallic region with the probe molecule present. Fig. 2(b) inset shows an optical transmission image of the Ag arraypatterned substrate and also the substrate with Ag absent. The experimental system used enabled optical transmission images to be recorded *in situ* with Raman scattering spectra, allowing precise, spatially resolved Raman scattering spectra to be obtained. Inspection of the luminescence spectrum shows that maximum luminescence intensity occurs at ca. 550 nm. The luminescence spectrum shows Raman scattering bands superimposed. The luminescence spectrum of $LiNbO_3$ substrate + Rh6G was recorded. Comparing the luminescence intensity from each of the two substrates shows that a ca. 4-fold increase in luminescence occurs when Ag is present, i.e., SEL occurs.

Raman scattering and luminescence spectroscopy of a second probe molecule were performed on $LiNbO_3$ + Ag nanopattern + Rubpy. Rubpy molecule was studied which luminesces at ca. 700 nm, a spectral region separated from the observed Raman scattering, which is centred at ca. 590 nm using $\lambda_{ex} = 532$ nm. The resulting Raman scattering spectrum is shown in Fig. 2(c-α). Raman scattering spectroscopy of $LiNbO_3$ substrate + probe molecule was also recorded showing no Raman scattering features originating from Rubpy (see Fig. 2(c-β)). As for the Rh6G dye, negligible peak intensity is present on the background compared to when Ag is present indicating that the Ag enhances the Raman scattering efficiently, i.e., SERS is observed for both probe molecules on the Ag.

Luminescence spectroscopy was performed on $LiNbO_3$ + Ag nanopattern + Rubpy. The resulting luminescence spectrum is shown in Fig. 2(d-α). The luminescence spectrum shows a broad band maximizing at ca. 675 nm. Recording the luminescence off the silver by positioning the probe laser away from the Ag nanopatterned arrays, probing only the $LiNbO_3$ substrate + Rubpy, was performed. The resulting luminescence spectrum is shown in Fig. 2(d-β). This spectrum shows a broad band maximizing at ca. 700 nm. The presence of the Ag nanopatterned array creates a "blue-shift" in the emission. Studies of Rhodamine Red with silver nanoparticle overlayers reported a significant "blue-shift" of the luminescence spectrum compared to when Ag is absent.[30] The authors reported that the presence of the Ag enables a borrowing of oscillator strength from the silver plasmon resonance through a dipolar coupling mechanism. The absorption maximum of the plasmon absorption for the Ag nanopatterned arrays is ca. 550 nm, i.e., to the blue of the luminescence from the probe molecule (see Fig. 1(c)). Fig. 2(d) shows that the luminescence from the Ag nanopatterned arrays is greater by ca. 20% than the luminescence from the same probe molecule on $LiNbO_3$ substrate in absence of Ag. This indicates that SEL occurs with Rubpy, albeit to a much lower extent than for Rh6G.

It is noted that the luminescence intensity for Rubpy on Ag is increased by a modest amount ca. 20%, this may be due to the coupling efficiency of the probe molecule in regard to coupling with the Ag. Effects such as aggregation may lead to a reduction in this efficiency as only Rubpy molecules in contact with Ag result in SERS. Such aggregation may shield molecules from effective coupling with the surface plasmon polaritons (SSP). However, it is noted that the observed "blue-shift" indicates that a large number of the probe molecules may be coupled with the surface plasmons. The surface plasmon resonance for the Ag is to the "blue" of the Rubpy emission by ca. 150 nm, meaning that coupling of the SSPs with photons at the luminescence wavelengths is inefficient compared to when a probe molecule (i.e., Rh6G) with emission nearer 550 nm is used. For Rubpy, low SEL is expected since only a small overlap exists between luminescence absorption and emission with the plasmonic absorption band of the substrate.[31] In contrary, a great enhancement is expected for Rh6G since a significant overlap exists between the luminescence absorption, emission and plasmonic absorption.[32,33]

The Raman scattering and luminescence spectra recorded for probe molecules on the Ag nanopatterned array show surface enhancement of luminescence and Raman scattering. Studies were performed to assess the SERS reproducibility over the substrate by recording the Raman scattering spectrum over a number of points. The Raman scattering intensity (normalised) recorded over ca. 30 μm for 6 points on a Ag nanopattern is plotted in Fig. 3(a). Inset in Fig. 3(a) shows the optical transmission image indicating the location of where the Raman scattering was recorded. The plot of Raman scattering intensity vs. position shows that the SERS intensity varies by less than 7% across the substrate.

Examination of the luminescence from the Rubpy sample was undertaken using FLIM (see Fig. 3(b)). The FLIM imaging of the Ag nanopatterned array shows features similar to those seen in the AFM topography image for the array

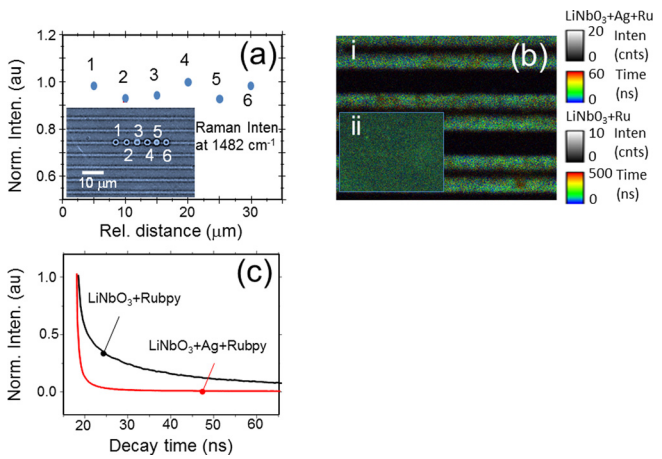

FIG. 3. (a) Variation in SERS intensity over 6 points on a single Ag nanostructure as shown in inset. (b) (i) False colour FLIM image of $LiNbO_3$ substrate + Ag nanopattern + Rubpy, (ii) Li substrate + Rubpy. Shown are scale bars for emission intensity (grey scale) and fluorescence decay time (coloured scale) both superimposed and displayed together. (c) Normalized decay traces taken from (b-i) and (b-ii).

(see Fig. 3(b)). The lifetime recorded for the probe dye (Rubpy) was <60 ns on the Ag arraypatterned substrate. This compares to the lifetime for the probe molecule on the $LiNbO_3$ substrate which was <500 ns (as shown in Fig. 3(b)). When Ag is absent, the FLIM image shows no distinct features apart from a uniform colour arising from the presence of the probe molecule evenly coated over the substrate. Fig. 3(c) shows a decay plot for Rubpy on the Ag arraypatterned substrate and on the $LiNbO_3$ substrate. The lifetime for the probe molecule on the substrate in absence of Ag is on average 127 ns. When Ag is present, the exciton recombination time for the probe molecule is reduced to on average 28 ns. This decrease in lifetime is related to metal induced quenching and enhancement mechanisms between the Ag nanopatterned array and probe molecule.[34] Further enhancement can be achieved with a spacer layer between metal and probe molecule, thereby eliminating metal induced quenching of the luminescence.[34]

Calculations of the plasmonic properties of the nanopatterned array were undertaken. Calculation of the electric field distribution at the silver-air interface was done via COMSOL by finite element analysis using RF module and excitation using background field of 1 V/m in field strength. The calculations were made in 2D with an electromagnetic (EM) wave incident on the silver from below with an electric field polarized along the nanopattern array. The wave was modified in COMSOL using the dielectric properties of $LiNbO_3$. The dielectric properties of silver were obtained from Johnson and Christy.[35] Earlier studies of proton exchange directed self-assembly of silver nanoparticles into nanopatterned arrays by Damm *et al.*[22] demonstrated that variations in height of the nanopatterns surface were present leading to significant electric fields in the region associated with SERS. The calculations are based on the rough surface (supported by AFM topography measurements) created by Ag nanoparticles. Calculations show that excitation wavelength in the blue causes the highest enhancement, while excitation in the red causes a relatively low enhancement. These calculations are in line with experimental findings where a significant enhancement in luminescence occurs at 550 nm (for Rh6G) compared to when a luminescent dye at 700 nm is used, i.e., Rubpy, where relatively poor enhancements of the luminescence signal was found. However, it is noted that sample preparation, location of the fluorophore, and other parameters will contribute to the observed enhancements.

Ag nanopatterned arrays prepared using periodically proton exchanged templates were demonstrated to support SEL. Fluorescence lifetime imaging revealed that fluorescence intensity is greatest on Ag and that the molecular probes lifetime was reduced in line with a surface enhanced luminescence mechanism. Studies showed that the substrate simultaneously supports SEL and SERS. Fluorophores emitting near the plasmon absorption maxima were enhanced 4-fold. Fluorphores that emit to the red of the plasmon absorption band were "blue-shifted" potentially via a dipolar coupling mechanism.

This work was supported by grants from Science Foundation Ireland (SFI). The Nanophotonics and Nanoscopy Research Group is supported by SFI Grant Nos. 11/RFP.1/MTR/3151, 12/IP/1556, and 09/RFP/PHY2398.

[1]E. Fort and S. Gresillon, J. Phys. D: Appl. Phys. **41**, 013001–013009 (2008).
[2]W. E. Smith, Chem. Soc. Rev. **5**, 955–964 (2008).
[3]F. Lordan, J. H. Rice, B. Jose, R. J. Forster, and T. E. Keyes, Appl. Phys. Lett. **97**, 153110–153113 (2010).
[4]F. Lordan, J. H. Rice, B. Jose, R. J. Forster, and T. E. Keyes, Appl. Phys. Lett. **99**, 033104–033107 (2011).
[5]F. Lordan, J. H. Rice, B. Jose, R. J. Forster, and T. E. Keyes, J. Phys. Chem. C **116**, 1784–17898 (2012).
[6]F. Lordan, N. Al-Attar, C. Mallon, J. Bras, G. Collet, R. J. Forster, T. E. Keyes, and J. H. Rice, Chem. Phys. Lett. **556**, 158–162 (2013).
[7]F. Lordan, S. Damm, N. Al-Attar, C. Mallon, R. J. Forster, T. E. Keyes, and J. H. Rice, "The Effect of Ag Nanoparticles on Surface-Enhanced Luminescence from Au Nanovoid Arrays," Plasmonics (published online).
[8]X. Zhao, F. Pan, H. Xu, M. Yaseen, H. Shan, C. A. E. Hauser, S. Zang, and J. R. Lu, Chem. Soc. Rev. **39**, 3480–3489 (2010).
[9]J. C. Huie, Smart Mater. Struct. **12**, 264–269 (2003).
[10]R. A. Taylor, J. W. Robinson, J. H. Rice, A. Jarjour, J. D. Smith, R. A. Oliver, G. A. D. Briggs, M. J. Kappers, C. J. Humphreys, and Y. Arakawa, Physica E **21**, 285–289 (2004).
[11]J. H. Na, R. A. Taylor, J. H. Rice, J. W. Robinson, K. H. Lee, Y. S. Park, C. M. Park, and T. W. Kang, Appl. Phys. Lett. **86**, 083109–083112 (2005).
[12]L. Qian and R. Mookherjee, Nano Res. **4**, 1117–1122 (2011).
[13]R. W. Martin, P. R. Edwards, R. A. Taylor, J. H. Rice, J. H. Na, J. W. Robinson, J. D. Smith, C. Liu, and I. M. Watson, Physica Status Solidi A **202**, 372–374 (2005).
[14]J. H. Rice, R. A. Oliver, G. A. D. Briggs, M. J. Kappers, C. J. Humphreys, J. D. Smith, and R. A. Taylor, Physica E **21**, 546–549 (2004).
[15]D. Li and D. A. Bonnell, Annu. Rev. Mater. Res. **38**, 351–366 (2008).
[16]S. V. Kalinin, D. A. Bonnell, T. Alvarez, X. Lei, Z. Hu, and J. H. Ferris, Nano Lett. **2**, 589 (2002).
[17]J. N. Hanson, B. J. Rodriguez, R. J. Nemanich, and A. Gruverman, Nanotechnology **17**, 4946 (2006).
[18]J. L. Jackel and C. E. Rice, Ferroelectrics **38**, 801–804 (1981).
[19]N. C. Carville, M. Manzo, S. Damm, M. Castiella, L. Collins, D. Denning, S. A. L. Weber, K. Gallo, J. H. Rice, and B. J. Rodriguez, ACS Nano **6**, 7373–7380 (2012).
[20]F. Merola, S. Grilli, S. Coppola, V. Vespini, S. De Nicola, P. Maddalena, C. Carfagna, and P. Ferraro, Adv. Funct. Mater. **22**, 3267–3272 (2012).
[21]Y. Cho, K. Fujimoto, Y. Hiranaga, Y. Wagatsuma, A. Onoe, K. Terabe, and K. Kitamura, Appl. Phys. Lett. **81**, 4401–4404 (2002).
[22]S. Damm, N. C. Carville, B. J. Rodriguez, M. Manzo, K. Gallo, and J. H. Rice, J. Phys. Chem. C **116**, 26543–26550 (2012).
[23]X. Liu, H. Hatano, S. Takekawa, F. Ohuchi, and K. Kitamura, Appl. Phys. Lett. **99**, 053102–053105 (2011).
[24]X. Liu, K. Kitamura, K. Terabe, H. Hatano, and N. Ohashi, Appl. Phys. Lett. **91**, 044101–044106 (2007).
[25]Z. Shen, G. Chen, Z. Chen, X. Qu, Y. Chen, and R. Liu, Langmuir **27**, 5167–5174 (2011).
[26]A. Haussmann, P. Milde, C. Erler, and L. M. Eng, Nano Lett. **9**, 763 (2009).
[27]S. Dunn and D. Tiwari, Appl. Phys. Lett. **93**, 092905 (2008).
[28]Y. Sun, B. S. Eller, and R. J. Nemanich, J. Appl. Phys. **110**, 084303–084310 (2011).
[29]M. Manzo, F. Laurell, V. Pasiskevicius, and Katia Gallo, Appl. Phys. Lett. **98**, 122910 (2011).
[30]S. Pan, Z. Wang, and L. J. Rothberg, J. Phys. Chem. B **110**, 17383–17387 (2006).
[31]B. Jose, R. Steffen, U. Neugebauer, E. Sheridan, R. Marthi, R. J. Forster, and T. E. Keyes, Phys. Chem. Chem. Phys. **11**, 10923–10933 (2009).
[32]A. Santhi, M. Umadevi, V. Ramakrishnan, P. Radhakrishnan, and V. P. N. Nampoori, Spectrochim. Acta, Part A **60**, 1077–1083 (2004).
[33]L. Dolgov, V. Reedo, V. Kiisk, S. Pikker, I. Sildos, and J. Kikas, Opt. Mater. **32**, 1540–1544 (2010).
[34]C. D. Geddes and J. R. Lakowicz, J. Fluoresc. **12**(2), 121–129 (2002).
[35]P. B. Johnson and R. W. Christy, Phys. Rev. B **6**, 4370–4379 (1972).